JOURNAL OF Materials CHEMISTRY

Soft solution processing for fabrication of lithiated thin-film electrodes in a single synthetic step

Kyoo-Seung Han, Petr Krtil and Masahiro Yoshimura*

Center for Materials Design, Materials and Structures Laboratory, Tokyo Institute of Technology, 4259 Nagatsuta, Midori, Yokohama 226, Japan. E-mail: yoshimu1@rlem.titech.ac.jp

A process called 'soft solution processing' was used to prepare lithiated thin-film electrodes as a cathode for lithium rechargeable microbatteries in a single synthetic step. The well crystallized $Li_{1-x}Ni_{1+x}O_2$ films were fabricated by the electrochemical–hydrothermal treatment of nickel plates in 4 M LiOH solution at fixed temperatures around 100 °C with no post-synthesis annealing. The prepared films exhibit prospective electrochemical activity; however, it is dependent on the synthetic conditions. The film formation mechanism study elucidates the effect of the synthetic conditions and also shows that soft solution processing is capable of preparing advanced inorganic materials with desired properties through the active control of the reaction conditions.

Advances in the miniaturization of electronic devices have triggered the efforts of many solid state chemists, electrochemists, and material scientists to develop suitable microbattery systems as power sources for microelectronics. In this way, all-solid-state lithium ion rechargeable microbatteries have attracted great interest, because they have improved many problems of secondary microbatteries while retaining most of their favorable features.[1–6]

The major difficulty in fabricating these microbatteries is ascribed to the ability to prepare lithiated intercalation cathode films. The experimental approach described in previous studies to fabricate thin-film positive electrodes has been focused primarily on the usage of gas phase and/or vacuum systems, such as chemical vapor deposition (CVD) and sputtering.[1–8] It should be noted how difficult it is to form a gas phase from a solid-state lithiated ternary oxide in these methods. Such syntheses therefore represent highly sophisticated multistep fabrication procedures, which unfortunately require high energy consumption, expensive precursors and equipment as well as post-synthesis heat treatments to obtain satisfactory electrochemical activity. Each of these techniques might result in environmental and economic problems. In fact, although intensive attention has been focused on the fabrication of long-lasting and high energy density microbatteries, the economic, environmental and energy factors of the fabrication processes have not been adequately considered. A recent life cycle analysis revealed that the fabrication process of a lithiated cathode used up to 80% of the total energy to fabricate a battery.[9] Therefore, it is important to develop a novel economical, environmentally friendly, and less energy-consuming process that can produce the desired lithiated intercalation cathode films on a chip. This would require the novel synthetic approach first to decrease the number of synthetic steps and second to be highly compatible with the electronic components. Soft solution processing seems to fit these criteria.[10–18] 'Soft solution processing' is a term encompassing a wide group of synthetic processes used to prepare inorganic materials using solution treatment at low temperature. The solution treatment of the starting material is often combined with different activation methods such as electrochemical reactions, photochemical excitation, application of microwaves, or hot-pressing to prepare the desired materials.[11–14,19–23] Here, we present the results of the successful fabrication of $Li_{1-x}Ni_{1+x}O_2$ films in a single step using soft solution processing, as well as a good example of how to improve the desired material preparation by design of the experimental conditions based on the elucidation of the microstructuring mechanism. In addition, some possible consequences of the film formation mechanism study will be pointed out.

Experimental

Materials

Nickel plates (99.7%, Nilaco Co., Japan) were polished with 1.0 μm diamond paste, degreased with soap and rinsed with distilled water prior to the film fabrication. Lithium hydroxide (4.0 M) electrolytes were prepared from reagent grade lithium hydroxide monohydrate (Junsei Chemical Co., Japan) and doubly distilled water. All of the film preparations were carried out in a laboratory-made stainless steel autoclave with a PTFE vessel adapted to the pressure vessel. The temperature in the reaction vessel was regulated using an external heating system, a chromel–alumel thermocouple and an automatic controller. All electrochemical processes were performed in a three-electrode arrangement using Ni working and auxiliary electrodes and a temperature-controlled Ag/AgCl reference electrode.[24] The electrochemical transients were controlled using a Toho-Giken Potentiostat/Galvanostat 2000 (Toho-Giken Co. Japan). The electrochemical–hydrothermal experiments were carried out at a fixed temperature between 100 and 200 °C for 20 h. During the electrochemical–hydrothermal process, the Ni working electrode was galvanostatically charged at a fixed current density between 0.1 and 5.0 mA cm^{-2}. Prepared films were rinsed several times with doubly distilled water to eliminate residual LiOH solution and then dried with blowing air.

Film characterization

The X-ray photoelectron spectroscopy (XPS) spectra of the films were recorded after Ar sputtering for 30 seconds with a Shimadzu ESCA3200 using Mg-Kα radiation. Binding energy values were all referenced to the carbon 1s line taken as 285.0 ± 0.5 eV. The X-ray diffraction pattern analysis of the films was obtained using a MAC Science MXP-3VA diffractometer and Cu-Kα radiation ($\lambda = 1.5405$ Å) operated at 40 mA and 40 kV. The diffractograms were recorded in the 2θ range 10–120° with 0.02° resolution. For the thin-film X-ray diffraction pattern, a grazing angle of 1.0° was used. Two-probe AC impedance measurements (Hewlett-Packard 4284A impedance analyzer) for the frequency range between 20 Hz and 1 MHz were performed to evaluate the obtained film conductivity. The two probes were installed on the surface of the obtained films at a separation of 1.0 cm. A cyclic voltammo-

gram of the films was recorded to test their electrochemical activity using a PAR EG&G potentiostat/galvanostat 273A. The electrochemical characterization was performed in 0.1 M $LiClO_4$ propylene carbonate (potential is referred to the Li/Li^+ electrode) under Ar atmosphere. The surface images of the Ni substrate and the $LiNiO_2$ films were obtained using a PicoSPM MS300 scanning probe microscope (Molecular Imaging, USA), operating in contact mode in air with a S_3N_4 cantilever (cantilever force constant 0.38 N m^{-1}).

Results and Discussion

The cobalt-blue colored film that formed on the surface of the Ni substrate was subsequently analyzed with respect to its structure, composition and crystallinity. The XPS data of the fabricated film confirmed the presence of both lithium and trivalent nickel in the film [Fig. 1(A) and (B)]. The Li/Ni molar ratio in the film, extracted from the XPS spectra, was close to 1, which is in accordance with expected stoichiometry. In the X-ray diffractogram [Fig. 2(A) and (B)] measured in the thin layer arrangement, X-ray diffraction (XRD) peaks characteristic of the lithium nickel oxide phase can be distinguished from those of the Ni substrate.[25] The prepared film shows good crystallinity despite the relatively low fabrication temperature without any post-synthesis annealing. Here, it is necessary to note that stoichiometric and non-stoichiometric lithium nickel oxide phases with different lithium and nickel contents as well as different nickel valences have been reported,

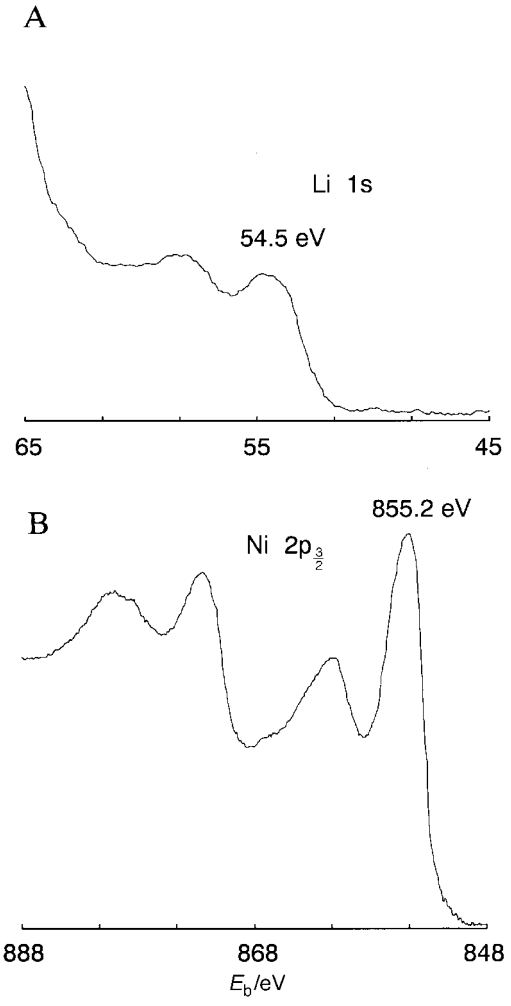

Fig. 1 X-Ray photoelectron spectroscopy (XPS) data for the film prepared by electrochemical–hydrothermal treatment of a Ni plate in 4 M LiOH solution at 150 °C with a current density of 1.0 mA cm^{-2}: (A) Li 1s XPS spectrum, (B) Ni $2p_{3/2}$ XPS spectrum

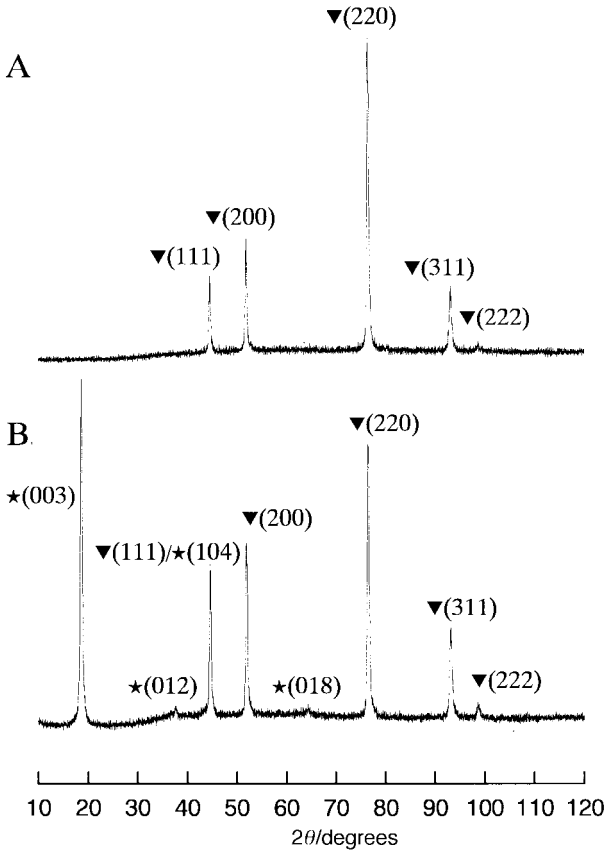

Fig. 2 X-Ray diffraction patterns for (A) Ni metal substrate and (B) the prepared film. Peaks denoted by ★ are assigned to $Li_{1-x}Ni_{1+x}O_2$; peaks denoted by ▼ are assigned to Ni substrate.

such as layered (space group $R\bar{3}m$), spinel (space group $Fd3m$), and rock-salt type (space group $Fd3m$ or $Fm\bar{3}m$ depending on the random cation ordering) lithium nickel oxides.[25–31] In addition, their X-ray diffraction patterns are unfortunately quite similar. As is well known, the ideal composition $LiNiO_2$ is difficult to prepare even by solid-state synthesis at any temperature. Although the obtained XPS and XRD data are not conclusive evidence for the exact chemical composition, it is evident that lithium nickel oxide ($Li_{1-x}Ni_{1+x}O_2$) films are fabricated during the electrochemical–hydrothermal reaction. Another indirect piece of evidence for the characterization of the prepared film is the fact that it has ionic conductivity and electrochemical activity. Considering the nature of lithium nickel oxide, the semicircle at high frequencies in the Cole–Cole plot of the fabricated film (Fig. 3) may correspond to its ionic conductivity. However, it is hard to determine whether the semicircle comprises either two overlapping semicircles or one semicircle depressed and shifted to negative Z'' values. In the latter case, the shift may be attributed to a conduction effect. According to the cyclic voltammograms (Fig. 4), the prepared film can be electrochemically oxidized and reduced in 0.1 M $LiClO_4$ propylene carbonate solutions. Additional information on the structure of the prepared film can be obtained from its electrochemical activity. While both layered and spinel lithium nickel oxides exhibit electrochemical activity, it is considered that rock-salt type lithium nickel oxide will not since the Li and Ni atoms in rock-salt type lithium nickel oxide randomly occupy its octahedral cationic sites. The peak potentials characterizing both the oxidation (*ca.* 4.0 V) and reduction (*ca.* 3.3 V) processes are similar to those for a layered $LiNiO_2$ powder electrode.[32] Another oxidation peak above 4.3 V may be associated with the decomposition of propylene carbonate and/or the oxidation of trivalent nickel to tetravalent nickel.

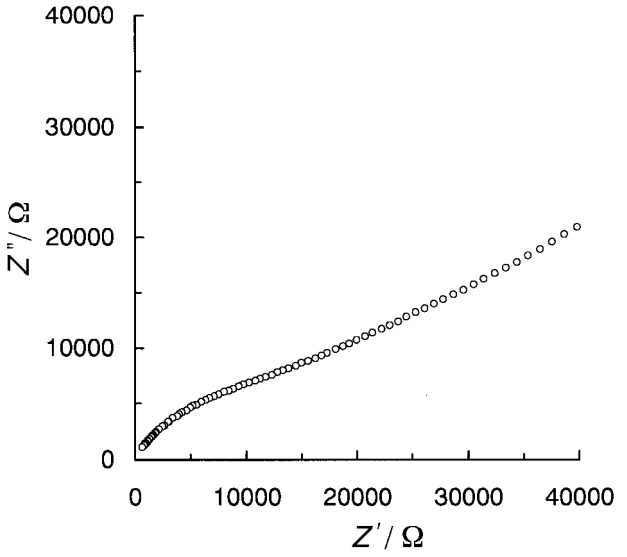

Fig. 3 Cole–Cole plot of the $Li_{1-x}Ni_{1+x}O_2$ film prepared at 150 °C with a current density of 1.0 mA cm^{-2}

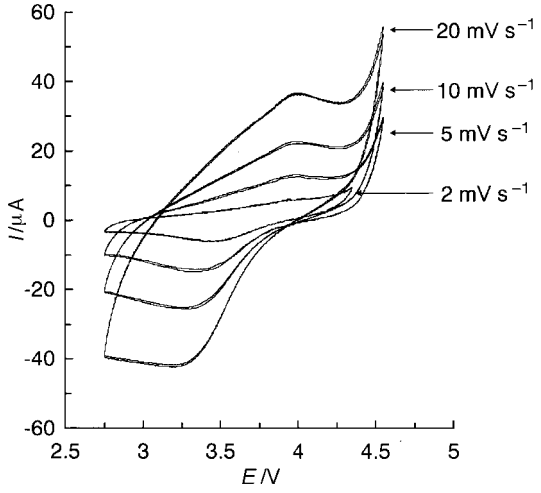

Fig. 4 Cyclic voltammograms of the $Li_{1-x}Ni_{1+x}O_2$ film prepared at 150 °C with a current density of 1.0 mA cm^{-2} taken in 0.1 M $LiClO_4$ propylene carbonate (potential is referred to the Li/Li^+ electrode) at various scan rates

Unfortunately, a more detailed analysis of the oxidation above 4.3 V is prevented owing to the decomposition of electrolytes at high potentials. In addition, as can be expected, the precise peak positions for the oxidation and reduction processes move towards more positive and negative currents respectively, with increasing scan rate (Fig. 5). Such a shift may be attributed to uncompensated resistance within the whole electrode. In Fig. 5, the peak currents show a relatively linear dependence on the square root of the scan rate. Such behavior is generally expected for a diffusion controlled electrode process. The diffusion coefficients extracted from the dependence were almost the same for the anodic and cathodic processes, with a value of 10^{-11} cm^2 s^{-1}. Though this value is roughly estimated due to the small departure from linearity of the I_p *vs.* $v^{1/2}$ line, it is comparable with the literature values of 10^{-14}–10^{-10} cm^2 s^{-1} for $LiCoO_2$ and $LiMn_2O_4$ films prepared by deposition methods.[2,3,33] Though detailed characterization of the properties of the obtained films, such as battery performance, is necessary, it is difficult when the obtained $Li_{1-x}Ni_{1+x}O_2$ films are on the surface of the Ni metal substrates. Ni metal plate can be oxidized at around 2.78 V *vs.*

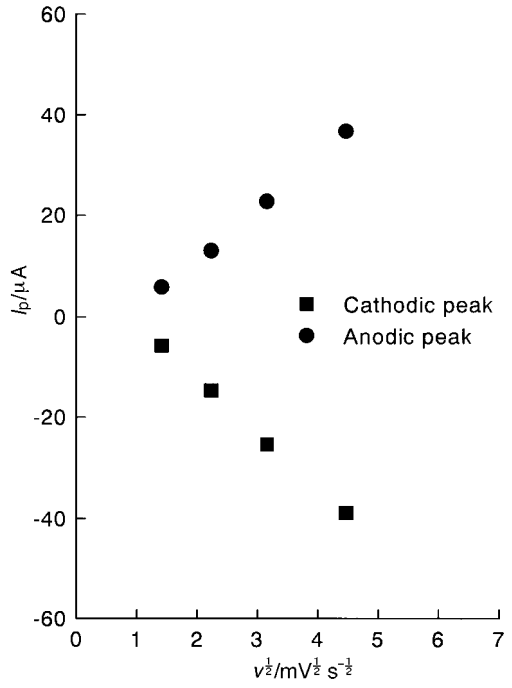

Fig. 5 Dependence of the peak current on the square root of scan rate for the $Li_{1-x}Ni_{1+x}O_2$ film prepared at 150 °C with a current density of 1.0 mA cm^{-2}

Li/Li^+, which will affect the electrochemical properties of the obtained $Li_{1-x}Ni_{1+x}O_2$ films. In addition, the films prepared at different temperatures show different electrochemical activity (Fig. 6), which indicates the importance of the synthesis conditions and their influence on the reaction mechanism. Similarly, the effect of fabrication temperature on the surface morphology [Fig. 7(A)–(F)] and film thickness (Fig. 8) was detected from atomic force microscope (AFM) surface images and scanning electron microscope (SEM) cross-sectional views, respectively. The film thickness and the grain size calculated from the AFM surface images as a function of fabrication temperature do not change at a fixed rate but exhibit a local maximum at 125 °C. The maximum itself might be assigned to

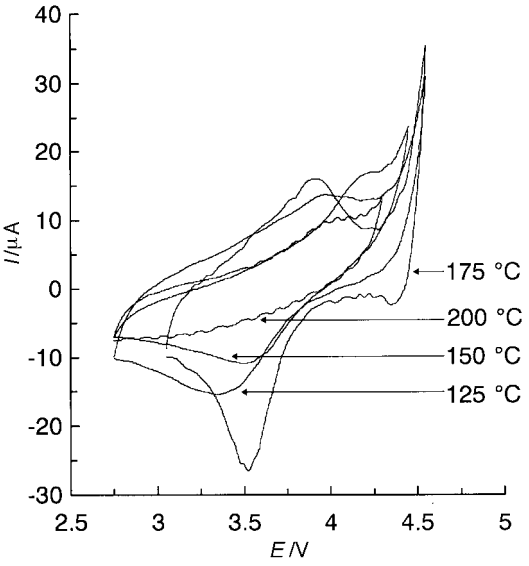

Fig. 6 Cyclic voltammograms of the $Li_{1-x}Ni_{1+x}O_2$ films prepared at different temperatures with a current density of 1.0 mA cm^{-2} taken in 0.1 M $LiClO_4$ propylene carbonate (potential is referred to the Li/Li^+ electrode) with a scan rate of 10 mV s^{-1}

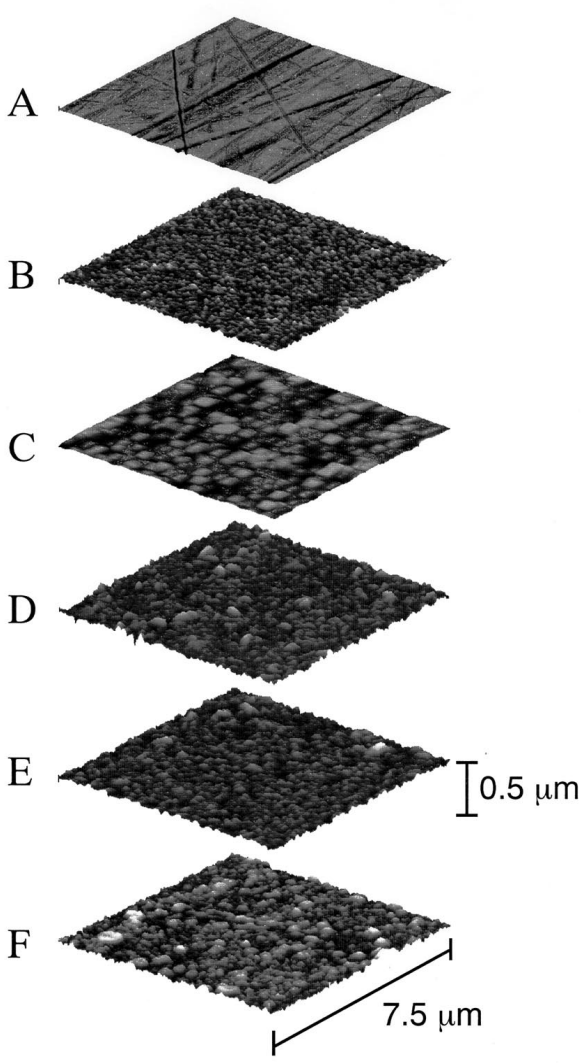

Fig. 7 Atomic force microscope (AFM) images of Ni substrate polished with 1.0 μm diamond paste and the $Li_{1-x}Ni_{1+x}O_2$ films prepared at different temperatures with a current density of 1.0 mA cm^{-2}. (A) Ni substrate, (B) the $Li_{1-x}Ni_{1+x}O_2$ film prepared at 100 °C, (C) the film prepared at 125 °C, (D) the film prepared at 150 °C, (E) the film prepared at 175 °C and (F) the film prepared at 200 °C.

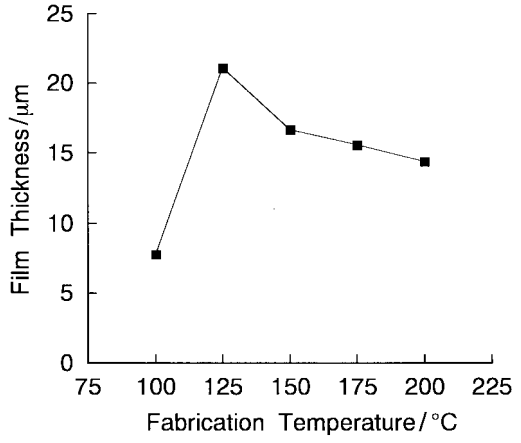

Fig. 8 Dependence of the film thickness on the fabrication temperature. The film thickness was evaluated from the scanning electron microscope (SEM) image of the sample cross section.

the occurrence of dissolution of the formed films as well as a change in the driving force for film formation which depends on temperature, which might lead eventually to a secondary dissolution of the films as represented in the following equation:

$$\partial C_i(x, y, z)/\partial t = D\nabla^2 C_i - k_1(1-\alpha)^m + k_2(1-\alpha)^n$$

where C_i denotes the concentration of reactant, D is the diffusion coefficient, k_1 and k_2 are kinetic constants of precipitation and secondary dissolution, respectively, and α is a supersaturation ratio.

According to the Pourbaix diagram,[34] one can propose three different reaction pathways to form the $Li_{1-x}Ni_{1+x}O_2$ film on the surface of the Ni substrate as shown in Fig. 9. Although precise representation of the actual reaction mechanism is prevented by the elevated fabrication temperature, at least qualitative information on the reaction pathway can be obtained from the time dependence of the potential of the Ni working electrode with respect to the Ag/AgCl reference electrode[24] during the electrochemical–hydrothermal treatment (Fig. 10). A glance at the potential curve shows four different stages. From this viewpoint, the most reasonable mechanism seems to be mechanism I in Fig. 9. In this pathway, the initial process is the formation of a $Ni(OH)_2$ film which corresponds to the part of the curve where the potential nears 0.5 V. In fact, it consists of two processes—oxidative dissolution and precipitation (Fig. 9). Because the product of the oxidative dissolution of the Ni substrate is a nickelite ion, the cell potential remains unchanged until the $Ni(OH)_2$ film starts to accumulate on the working electrode, leading eventually to a potential increase. The next process is characterized by a potential increase to around 1.0 V. It may correspond to another oxidation process that forms the NiOOH and/or $NiOOH_{1-x}\cdot H_2O$ film. As the final process, the cationic exchange reaction between H^+ and Li^+ as well as the dehydration of interlayer water to form the $Li_{1-x}Ni_{1+x}O_2$ film are

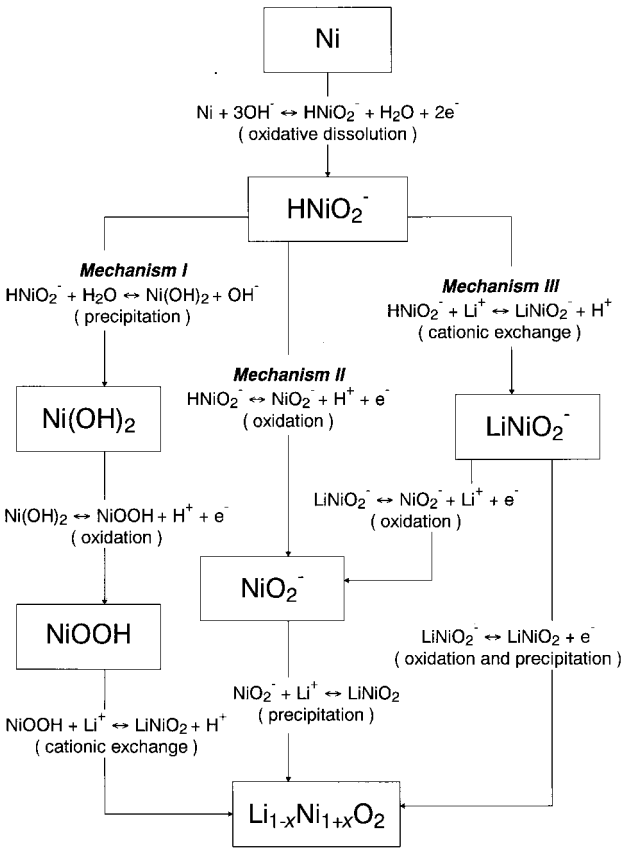

Fig. 9 Possible reaction pathways for $Li_{1-x}Ni_{1+x}O_2$ film formation proposed on the basis of the Pourbaix diagram

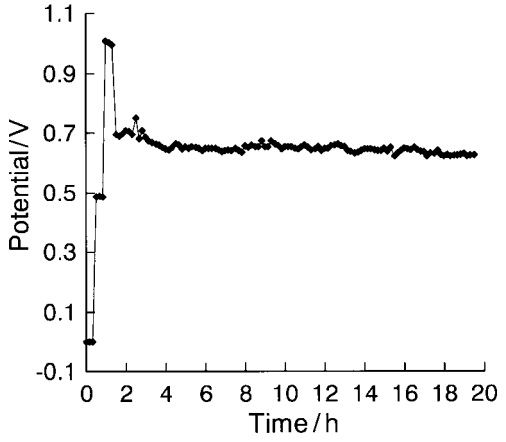

Fig. 10 Evolution of nickel electrode potential with respect to the Ag/AgCl reference electrode as a function of reaction time during electrochemical–hydrothermal treatment at 150 °C by galvanostatic oxidation at 3.0 mA cm^{-2}

subsequently characterized by a slow potential decrease to 0.7 V. It should be noted that while the nickel in $Ni(OH)_2$ and $Li_{1-x}Ni_{1+x}O_2$ film are divalent and almost trivalent respectively, those in NiOOH and/or $NiOOH_{1-x}\cdot H_2O$ films are considered to be higher than trivalent, even tetravalent.[35] Therefore, the evolution of potential during the whole process can be interpreted in terms of the variation of the nickel valency in the formed films. In addition, both above-mentioned intermediates can be isolated on the electrode (Fig. 11), if the polarization is interrupted at pre-selected potentials [0.5 V for $Ni(OH)_2$ and 1.0 V for NiOOH and/or $NiOOH_{1-x}\cdot H_2O$]. Once fabrication is resumed, a $Li_{1-x}Ni_{1+x}O_2$ film is formed as the final product. No intermediates other than $Ni(OH)_2$, NiOOH and $NiOOH_{1-x}\cdot H_2O$ were detected. The kinetics of each of the above-mentioned steps has a different temperature dependence; thus one can anticipate variation in the properties of the resulting films, such as electrochemical activity, film thickness, average particle size, *etc.*

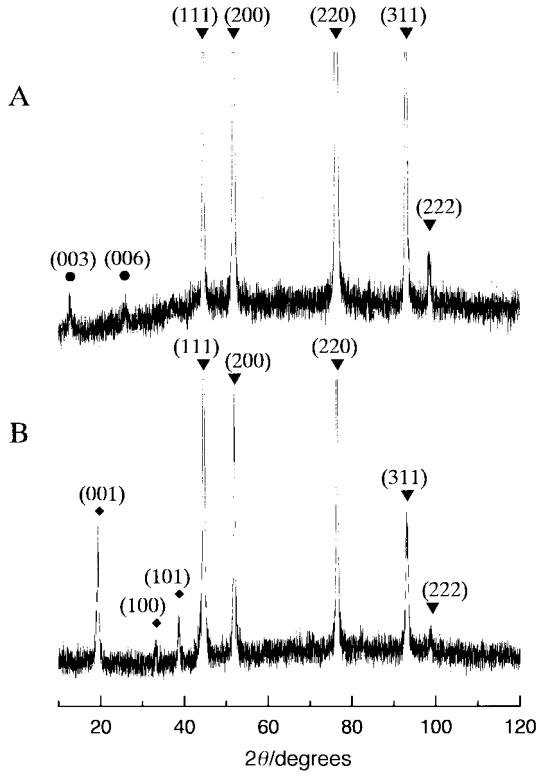

Fig. 11 X-Ray diffraction patterns for (A) $NiOOH_{1-x}\cdot H_2O$ film and (B) $Ni(OH)_2$ film. Peaks denoted by ▼ are assigned to Ni substrate; peaks denoted by ● are assigned to $NiOOH_{1-x}\cdot H_2O$; peaks denoted by ◆ are assigned to $Ni(OH)_2$.

Analysis of the film formation mechanism may not only be used to rationalize the difference in the final product properties, but it may also have a more general impact on the experimental approaches in the preparation of advanced inorganic material films. Though a detailed study of $Li_{1-x}Ni_{1+x}O_2$ film formation has still not been accomplished, we foresee the possibility that the properties of the $Li_{1-x}Ni_{1+x}O_2$ film can be controlled by actively changing the preparation conditions such as the applied current density, reaction time, concentration of the LiOH solution, *etc.* A supplemental set of individual electrochemical and hydrothermal experiments demonstrate that the desired $Li_{1-x}Ni_{1+x}O_2$ film can only effectively be prepared in a single synthetic step by a designed combination of the electrochemical anodic process (which induces the trivalent nickel) and hydrothermal treatment (which causes the cationic exchange reaction). The above-mentioned concepts apply not only to $Li_{1-x}Ni_{1+x}O_2$ and other materials for microbatteries or electrochromic devices but also possibly to other areas of materials research.

Conclusion

Well crystallized and electrochemically active $Li_{1-x}Ni_{1+x}O_2$ thin-film electrodes were fabricated in a single synthetic step in 4 M LiOH solution at fixed temperatures around 100 °C without any post-synthesis annealing. The implementation of soft solution processing to form lithiated thin-film electrodes shows a successful example of how to improve desired material preparation by the design of experimental conditions based on the elucidation of the microstructuring mechanism.

This work was supported by the 'Research for the Future' program of the Japan Society for the Promotion of Science (JSPS-RFTF-96R06901). The authors would like to thank Messrs. S. Tsurimoto, J. H. Lee, T. Watanabe, S. McLennan, K. Zimmer, W. Drake and K. Yamaura as well as Drs. S. H. Chang, M. Tabuchi, Z. Wu and J. Frantti for their help and discussion.

References

1 F. K. Shokoohi, J. M. Tarascon, B. J. Wilkens, D. Guyomard and C. C. Chang, *J. Electrochem. Soc.*, 1992, **139**, 1845.
2 P. Birke, W. F. Chu and W. Weppner, *Solid State Ionics*, 1997, **93**, 1.
3 K. A. Striebel, C. Z. Deng, S. J. Wen and E. J. Cairns, *J. Electrochem. Soc.*, 1996, **143**, 1821.
4 S. J. Lee, J. K. Lee, D. W. Kim, H. K. Baik and S. M. Lee, *J. Electrochem. Soc.*, 1996, **143**, L268.
5 K. H. Hwang, S. H. Lee and S. K. Joo, *J. Electrochem. Soc.*, 1994, **141**, 3296.
6 F. K. Shokoohi, J. M. Tarascon and B. J. Wilkens, *Appl. Phys. Lett.*, 1991, **59**, 1260.
7 M. Antaya, K. Cearns, J. S. Preston, J. N. Reimers and J. R. Dahn, *J. Appl. Phys.*, 1994, **76**, 2799.
8 M. Antaya, J. R. Dahn, J. S. Preston, E. Rossen and J. N. Reimers, *J. Electrochem. Soc.*, 1993, **140**, 575.
9 *Rare Metal News (Japan)*, 1997, **1867**, 2.
10 Y. G. Gogotsi and M. Yoshimura, *Nature*, 1994, **367**, 628.
11 M. Yoshimura, S. E. Yoo, M. Hayashi and N. Ishizawa, *Jpn. J. Appl. Phys.*, 1989, **28**, L2007.
12 K. Kajiyoshi, Y. Hamaji, K. Tomono, T. Kasanami and M. Yoshimura, *J. Am. Ceram. Soc.*, 1996, **79**, 613.
13 K. Kajiyoshi, M. Yoshimura, Y. Hamaji, K. Tomono and T. Kasanami, *J. Mater. Res.*, 1996, **11**, 169.
14 M. Yoshimura, W. Urushihara, M. Yashima and M. Kakihana, *Intermetallics*, 1995, **3**, 125.
15 W. S. Cho, M. Yashima, M. Kakihana, A. Kudo, T. Sakata and M. Yoshimura, *Appl. Phys. Lett.*, 1995, **66**, 1027.
16 W. S. Cho and M. Yoshimura, *Jpn. J. Appl. Phys.*, 1996, **35**, L1449.

17 M. R. Palacín, D. Larcher, A. Audemer, N. Sac-Épée, G. G. Amatucci and J. M. Tarascon, *J. Electrochem. Soc*., 1997, **144**, 4226.
18 M. Yoshimura and W. Suchanek, *Solid State Ionics*, 1997, **98**, 197.
19 S. Komarneni, R. Roy and Q. H. Li, *Mater. Res. Bull*., 1992, **27**, 1393.
20 S. Komarneni, Q. H. Li and R. Roy, *J. Mater. Chem*., 1994, **4**, 1903.
21 S. Komarneni, V. C. Menon, Q. H. Li, R. Roy and F. Ainger, *J. Am. Ceram. Soc. Commun*., 1996, **79**, 1409.
22 M. Yoshimura and S. Somiya, *Am. Ceram. Soc. Bull*., 1980, **59**, 246.
23 D. M. Roy and G. R. Gouda, *J. Am. Ceram. Soc*., 1973, **56**, 549.
24 D. D. Macdonald and D. Owen, *J. Electrochem. Soc*., 1973, **120**, 317.
25 L. D. Dyer, B. S. Borie Jr. and G. P. Smith, *J. Am. Chem. Soc*., 1954, **76**, 1499.
26 J. B. Goodenough, D. G. Wickham and W. J. Croft, *J. Phys. Chem. Solids*, 1958, **5**, 107.
27 G. Dutta, A. Manthiram, J. B. Goodenough and J. C. Grenier, *J. Solid State Chem*., 1992, **96**, 123.
28 W. Li, J. N. Reimers and J. R. Dahn, *Phys. Rev. B*, 1992, **46**, 3236.
29 M. G. S. R. Thomas, W. I. F. David, J. B. Goodenough and P. Groves, *Mater. Res. Bull*., 1985, **20**, 1137.
30 J. Morales, C. Perez-Vicente and J. L. Tirado, *Mater. Res. Bull*., 1990, **25**, 623.
31 J. R. Dahn, U. von Sacken and C. A. Michal, *Solid State Ionics*, 1990, **44**, 87.
32 M. Broussely, F. Perton, J. Labat, R. J. Staniewicz and A. Romero, *J. Power Sources*, 1993, **43–44**, 209.
33 C. H. Chen, E. M. Kelder, M. J. G. Jak and J. Schoonman, *Solid State Ionics*, 1996, **86–88**, 1301.
34 E. Deltombe, N. De Zoubov and M. Pourbaix, in *Atlas of Electrochemical Equilibria in Aqueous Solutions*, National Association of Corrosion Engineers, Houston, TX, 1974, nickel, section 12.3.
35 K. S. Han, M. Yoshimura, J. B. Yoon, J. H. Choy and K. J. Park, *J. Mater. Res*., 1998, **13**, 880.

Paper 8/04791J; *Received* 23*rd June*, 1998